

The twist-bend nematic phase: Translational self-diffusion and biaxiality studied by ^1H Nuclear Magnetic Resonance diffusometry

M. Cifelli^{a1}, V. Domenici^{a2}, S.V. Dvinskikh^{b,c3}, G.R. Luckhurst^{d4}, B.A. Timimi^{d5},

^aDipartimento di Chimica e Chimica Industriale, Università di Pisa, Italy

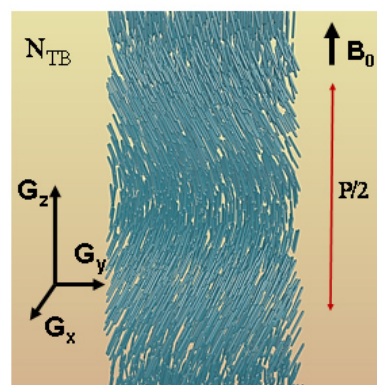
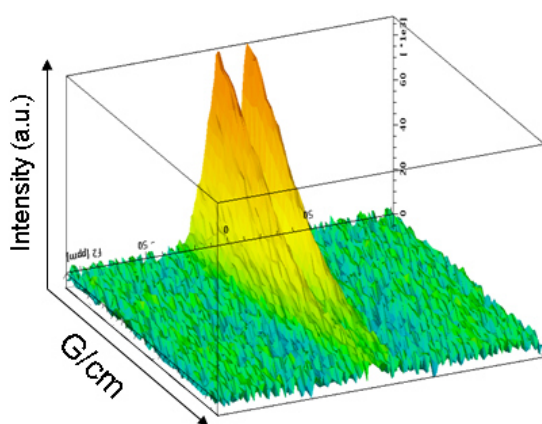
^bRoyal Institute of Technology, Department of Chemistry,
Teknikringen 36, SE-10044 Stockholm, Sweden.

^cSt. Petersburg State University, Laboratory of Biomolecular NMR,
St. Petersburg, 199034 Russia

^dChemistry, University of Southampton, Highfield, Southampton, SO17 1BJ, United Kingdom

ABSTRACT

Recently, there has been a surge of interest in mesogens exhibiting the twist-bend nematic (N_{TB}) phase that is shown to be chiral even though formed by effectively achiral molecules. Although it now seems to be clear that the N_{TB} phase in the bulk is formed by degenerate domains having opposite handedness, the presence of a supramolecular heliconical structure proposed in the Dozov model has been contradicted by the Hoffmann et al. model in which the heliconical arrangement is replaced by a polar nematic phase. The evidence in support of this is that the quadrupolar splitting tensor measured in various experiments is uniaxial and not biaxial as expected for the twist-bend nematic structure. In this debate, among other evidence, the molecular translational diffusion, and its magnitude with respect to that in the nematic phase above the N_{TB} phase, has been also invoked to eliminate or to confirm one model or the other. We attempt to resolve this issue by reporting the first measurements of the translational self-diffusion coefficients in the nematic and twist-bend nematic phases formed 1'',7''-bis-4-(4'-cyanobiphenyl) heptane (CB7CB). Such measurements certainly appear to resolve the differences between the two models in favour of that for the classic twist-bend nematic phase.



¹ corresponding author, email address: mario.cifelli@unipi.it

² email address: valentina.domenici@unipi.it

³ email address: sergeid@kth.se

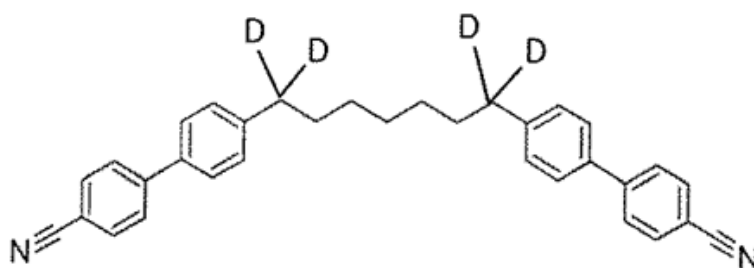
⁴ email address: G.R.Luckhurst@soton.ac.uk

⁵ email address: B.A.Timimi@soton.ac.uk

Keywords: twist-bend nematic, local phase biaxiality, molecular translational diffusion coefficients, macroscopic rotational diffusion, motional averaging, residual quadrupolar tensors

1. Introduction

The observation of a nematic-nematic phase transition for liquid crystal dimers where the spacer linking the two mesogenic groups contained an odd number of groups has proved, in the last few years to be of real interest. [1,2] The identity of the low-temperature nematic phase was not determined and so was denoted by N_X where the subscript X indicates that the phase identity was not known. However, a very detailed investigation of the two nematic phases exhibited by the odd liquid crystal dimer 1'',7''-bis-4-(4'-cyanobiphenyl-4'-yl) heptane (CB7CB)



allowed the low temperature nematic to be identified as the twist-bend nematic phase (N_{TB}). [3] In fact this phase was predicted first by Meyer [4] although it was largely ignored and then, a quarter of a century later, by Dozov; [5] the phase was predicted to have a heliconical structure with the director tilted with respect to the helix axis.

Despite experimental [6] and theoretical [7] support for the model of bent molecules arranged in short pitch helices proposed by Dozov, [5] the structure of the phase is still open to debate [8] and other theories have been suggested. [9,10] In particular, one of these excludes the presence of the helix in favour of a polar nematic phase with molecules distributed in domains with mirror symmetry. [9]

^2H NMR spectroscopy of CB7CB- d_4 , see the inserted structure for the location of the deuterons, played a major role in the identification of this phase chirality formed from essentially achiral molecules. In addition the residual quadrupolar splitting tensor measured in the twist-bend nematic phase was found to be uniaxial. This result is surprising in that the local symmetry of the N_{TB} phase is biaxial. However, the uniaxiality of the residual quadrupolar tensor has been confirmed for the higher homologue CB9CB- d_4 [11]. Similar behaviour has been observed for the chiral nematic phase where the helical structure should also induce phase biaxiality but this is not observed with NMR spectroscopy. [12,13] Here the explanation is that the biaxiality in the residual

magnetic tensors is averaged to zero by fast diffusion along the helix axis. Initially it was argued that such motional averaging could not occur for the twist-bend nematic because of its high viscosity. [11] To check this explanation it is clearly necessary to determine the translational diffusion coefficient along the helix axis. This experimental check seems to be essential since at present the debate is still open and relevant experimental efforts are being devoted on the one side to collect new evidence confirming one model with respect to the other and on the other side to discern a definitive relation between the molecular structure and the stable formation of the new phase. [14]

The presence of anisotropic translational mobility is a well-known, distinctive molecular property of liquid crystalline (LC) phases. One of the most direct experimental approaches with which to investigate translational diffusion in liquid crystals is Nuclear Magnetic Resonance Diffusometry.[15] A clear advantage of this technique is its direct access to the so-called self-diffusion coefficient, that is by measuring the Brownian diffusion of molecules forming the phase without having to use tracers and, equally being able to study the system at thermal equilibrium. Moreover, the presence of a high static magnetic field of several T offers an easy way to create a monodomain sample whose orientation with respect to the magnetic field depends on the diamagnetic susceptibility of the mesogen. This technique has been applied to different liquid crystalline phases and recently reviewed, in particular, for application to thermotropic liquid crystals. [16] Despite the different approaches proposed, the basic requirements are to have available hardware that allows the measurement of translational diffusion along different directions in the aligned sample and to exploit the experimental protocols that extend the transverse relaxation time toward its isotropic-phase value. More recent studies have concerned the investigation of translational diffusion at the smectic C^*_{ferro} – smectic $C^*_{\text{antiferro}}$ transition, [17,18] in re-entrant nematic phases [19] and ionic smectic liquid crystal phases. [20] Under favourable conditions, i.e. long transverse spin-relaxation times, diffusion coefficients as small as 10^{-13} m²/s have been measured. [17]

In the present paper we report the first measurements of the translational self-diffusion tensor in the nematic and twist-bend nematic phases formed by the nematogen CB7CB. Our aim is, therefore, to add to the molecular dynamic properties of the N_{TB} phase that can be related also to its supramolecular structure providing a contribution to its elucidation. In the next section the sample preparation and the basis of the pulse-field gradient methodology are described. The results of employing this to determine the parallel and perpendicular components of the diffusion tensor for the nematic and twist-bend nematic phase are given in Section 3. These and the diffusion anisotropy are discussed in the following section. Our conclusions are in Section 5. We also include two

appendices 1 and 2. The first describes the determination of the symmetry of the residual quadrupolar tensor for CB7CB-d₄ in the N_{TB} phase and the field-induced alignment of the symmetry axis in both the nematic and twist-bend nematic phases. In the second we describe the determination of the diffusometry experiments and their analysis, again in both nematic phases.

2. Experimental

2.1 CB7CB liquid-crystalline sample and ¹H NMR sample preparation

The protonated sample of CB7CB was prepared as described elsewhere [3]. For NMR measurements, the sample was loaded into a standard 5 mm glass tube and the sample height was limited to about 2 mm. This was to help reduce the temperature gradient and consequently thermal convection along the axis of the tube during the diffusion measurements.

2.2 Pulse field gradient (PFG) ¹H NMR method

NMR Diffusometry is a sound and well-established method to investigate molecular diffusion of fluids in general [21] and of liquid crystals in particular. [16] Combining spin-echo NMR with pulsed field gradients (PFG) of variable amplitude allows accurate measurement of diffusion coefficients along the gradient direction but avoiding side effects due to nuclear spin relaxation. Moreover, suitable choice and variation of the diffusion time also allows the investigation of deviations from the free-diffusion regime, such as spatial confinement in colloids [21] and diffusion restriction in micro-porous materials. [21] In liquid crystals, the anisotropy of the diffusion processes is related to molecular order, both orientational and positional, and so can be exploited to study the structure of the phases. For liquid crystal phases formed by mesogens with a positive magnetic susceptibility anisotropy ($\Delta\chi > 0$), the director tends to align parallel to the main magnetic field direction. If the alignment is homogeneous, application of the pulsed gradient along the laboratory frame axes allows measurements of the relevant diffusion coefficients with respect to the director.[16] In liquid crystals, the longitudinal spin relaxation time is much longer than the transverse one, hence the STimulated Echo (STE) pulse sequence is the best choice as its diffusion time is limited by the longer spin relaxation process. Due to the anisotropic character of the molecular mobility, the anisotropic spin interactions are, to a large extent, preserved in liquid crystals. Residual spin couplings (e.g. dipolar couplings for protons) strongly reduce the transverse

relaxation times, limiting the time window for the application of the pulsed gradients. In order to overcome this limitation, NMR pulse sequences have been developed which combine homonuclear decoupling with a PFG-STE experiment. Among the different homonuclear decoupling approaches, the magic echo (ME) spin decoupling for dipolar interaction was chosen as it provides larger time windows between radiofrequency (rf) decoupling pulses for inserting field gradient pulses. [16,17] The suitable combination of ME rf pulses and pulsed field gradients, as shown in Figure 1, allows the transverse relaxation time to be extended with a limited rf energy deposition on the sample with resultant negligible overheating. Moreover it allows the application of the gradient pulses in the absence of rf irradiation, thus avoiding distortions of the signal due to pulse interferences.

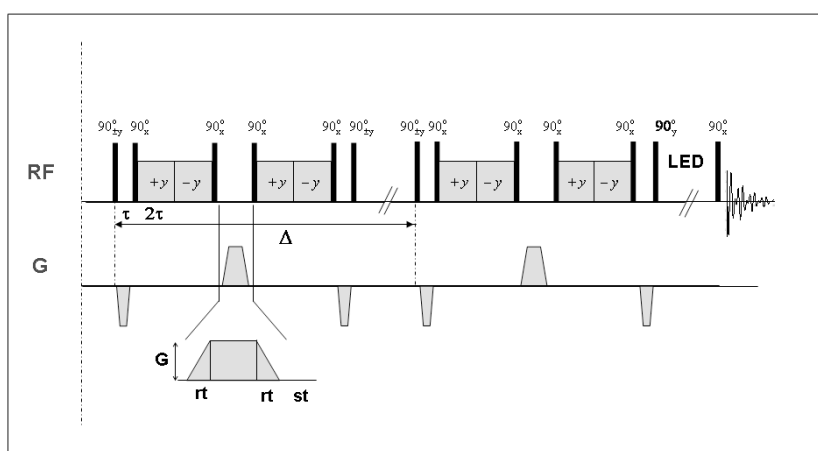


Figure 1. PFG STE-ME pulse sequence scheme. During the encoding/decoding time an ME decoupling sequence was inserted to extend the transverse relaxation time. Trapezoidal gradient shapes were used with a ramp time (rt) and a stabilization time (st) as discussed in the text. Bipolar gradient pulses were applied to achieve a cumulative effect of the field gradient. An LED delay was used to allow for the eddy current to decay prior to acquisition.

Self-diffusion measurements were performed on a Bruker Avance III 500 and a Bruker Avance II 300 spectrometer working at 500 MHz and 300 MHz frequency, respectively; that is with field strengths of 11.75 T and 7.05 T, respectively. A diffusion probe, Diff30, with a maximum field gradient of 1800 G/cm in the direction of the static field, and a micro-imaging probe, Mic5, having gradients of up to 290 G/cm in three orthogonal directions, have been used, retuning the rf coil at the suitable proton frequency. The 90° pulse width was 5.5 μs for both probes. Measurements in the isotropic phase have been carried out with a standard stimulated-echo sequence (STE), while in the nematic phases a STE combined with an ME spin decoupling sequence (STE-ME) was chosen (see Figure 1). ME decoupling delays, with $\tau = 260 \mu\text{s}$, were used to achieve significant diffusion decays of the stimulated echo over the whole temperature range investigated. Within these conditions the effective maximum gradient pulse length for the experiments, δ , was set to 0.56 ms with both Mic5 and Diff30 probes. The temperature stability during all of the experiments was $\pm 0.1 \text{ }^\circ\text{C}$.

Trapezoidal gradient shapes have been used with a short-ramp time and supplemented with stabilization delays (i.e. $rt = st = 50 \mu\text{s}$ and $100 \mu\text{s}$ for the Mic5 and Diff30 probes, respectively) long enough to avoid transient effects and interferences with rf pulses. To compensate for eddy-current fields, gradient waveforms were adjusted using the pre-emphasis method. Moreover, in experiments using the Diff30 probe the maximum gradient intensity was limited to 66% of the maximum value and shorter gradient pulses in the STE-ME sequence were removed leaving only the longer pulse. Finally, extension of the sequence with the Longitudinal Eddy current Delay (LED) period of 10 ms allowed for the suppression of the eddy-current effect during signal acquisition. [22]

The diffusion time (Δ , see Figure 1) was varied from 160 to 800 ms, while a longitudinal relaxation time, T_1 , was estimated to be about 1s in both phases. As reported in appendix 2, spectral shape of the STE-ME, retained the same features of the single pulse acquisition and the diffusion coefficient along the field-gradient direction was measured by fitting the decay dependence of the spectral signals (A) on the gradient strength leaving all of the time delays in the pulse sequence constant,

$$A(\gamma, \delta, G, \Delta) \propto \exp\left[-(\gamma\delta G)^2(\Delta - \delta/3)D\right], \quad (1)$$

Here γ is the nuclear gyromagnetic ratio, G is the gradient strength and D is the diffusion coefficient measured along the gradient direction.

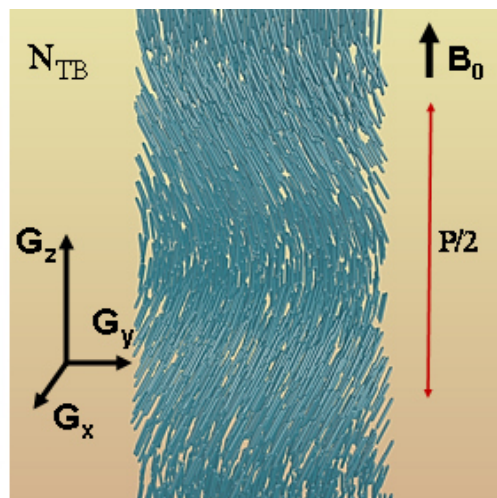


Figure 2 (colour online) Schematic representation of the twist-bend nematic phase aligned in the magnetic field, B_0 . The gradient reference frame used in the diffusion experiments, with the Z axis parallel to B_0 are also shown. (Modified with permission from [27])

3. Experimental Results

The director orientation in strong magnetic fields, typically of several T, has been investigated previously. [3,23,24] The nematic director is aligned parallel to the magnetic field, as expected for mesogens with $\Delta\chi>0$, while in the N_{TB} phase, the director tilts away from the helix axis which becomes the symmetry axis and is aligned along the field. [3] A schematic representation of the alignment of the structure in the twist-bend nematic phase is shown in Figure 2.

In experiments with field-gradient pulses along the Z direction, the diffusion coefficient $D_{//}$ is measured along the phase director and along the helix axis in the N and N_{TB} phases, respectively. To measure the diffusion coefficient D_{\perp} in the orthogonal direction, X or Y gradients, separately or combined, are applied.

In Figure 3 the translational-diffusion coefficient measured along different directions in the isotropic, nematic and twist-bend nematic phase are shown as a function of the inverse temperature. The results acquired at two different field strengths are shown as empty and full symbols corresponding to 11.75 T and 7.05 T, respectively. Here the aligning torques which are quadratic in the field acting on the directors differ by a factor of about 2.8. As shown in the figure, measurements acquired at the two different magnetic field strengths, show a remarkable agreement, indicating that the director alignment by the magnetic field, and the phase transition temperatures do not depend on the field strengths, for the cases employed.

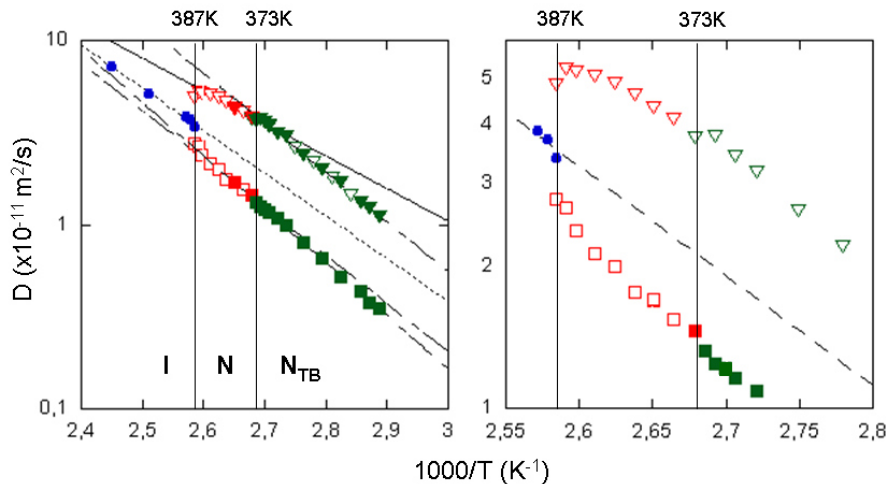


Figure 3. (colour online) Translational-diffusion coefficients measured in the isotropic (circles) and the nematic phases parallel $D_{//}$ (triangles) and perpendicular D_{\perp} (squares) to the magnetic field direction. Empty and full symbols represent diffusion coefficients measured at 11.75 T and 7.05 T, respectively. Lines represent fits to the Arrhenius equation, see text. On the right, the N - N_{TB} transition region is enlarged. For simplification a smaller but still significant number of experimental points are shown.

The good agreement between datasets acquired at different fields is also indication of high accuracy of the measurements; experimental error, evaluated from the standard deviation on three sets of measurements, two carried out at $B_0=11.75$ T and one at $B_0=7.04$ T can be framed between 2-4 % giving error bars corresponding to the dimensions of the symbol in the figure.

The isotropic-nematic phase transition is accompanied by the instant appearance of the anisotropy in the diffusion coefficient. The N – N_{TB} transition is less evident in the diffusion data, but can be identified by a small but significant increment (about 5%) in $D_{//}$ as shown in Figure 3. It is also clearly apparent as a jump in the quadrupolar splitting for CB7CB-d₄ [3] consistent with the first-order nature of this phase transition.

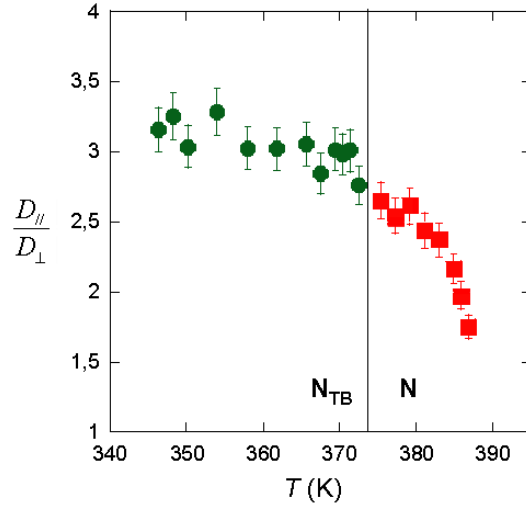


Figure 4. (colour online) The diffusion anisotropy in the nematic (■) and twist-bend nematic (●) phases shown as a function of temperature. Error bars come from error propagation from the experimental measured diffusion coefficients

4. Discussion

The self-diffusion behaviour in the nematic phase follows the relation $\frac{D_{//}}{D_{\perp}} > 1$ that increases as the temperature decreases, as shown in Figure 4. The N - N_{TB} transition can be identified by a discontinuous change of diffusion coefficients, in particular an increase in $D_{//}$. This discontinuous increase in the diffusion coefficient is consistent with a corresponding increase of the orientational order parameter for CB7CB-d₄ with respect to the phase director as the N_{TB} phase forms. [3] This feature is consistent with the ²H NMR behaviour of the deuteriated 8CB-d₂ probe dissolved in bulk CB7CB. [23]

The ratio of the diffusion coefficients, $\frac{D_{//}}{D_{\perp}} > 1$, while increasing steeply in the nematic phase

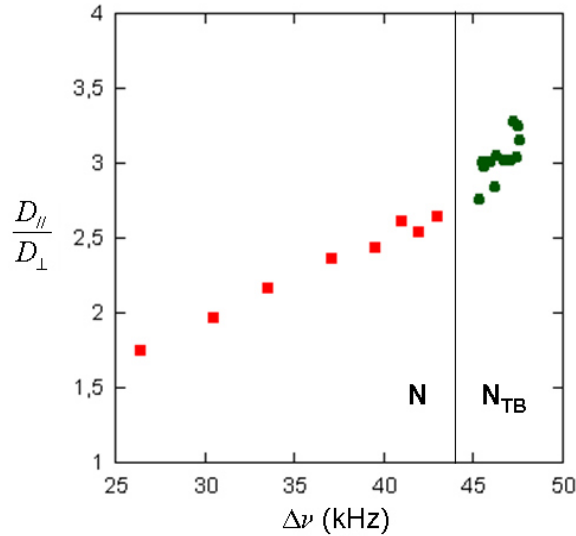


Figure 5. (colour online) A plot of the diffusion anisotropy, $D_{||}/D_{\perp}$, against the residual quadrupolar splitting, $\Delta\nu$, at the same temperatures, in the nematic (■) and the twist-bend nematic (●) phases.

with decreasing temperature and reaching a value of about 3, only changes slightly in the twist-bend nematic phase.

The temperature dependence of the diffusion anisotropy shown in Figure 4 bears a strong resemblance to that of the residual quadrupolar splitting, $\Delta\nu$, observed for CB7CB-d₄ (see Figure 13 [3]). Within the nematic phase the four deuterons are equivalent and the single quadrupolar splitting increases strongly with decreasing temperature. In contrast in the chiral twist-bend nematic phase the prochiral deuterons in a methylene group are inequivalent and while one splitting increases with decreasing temperature that of the other decreases. It is the mean of these prochiral splittings that is comparable to that in the nematic phase. At the N_{TB}-N phase transition there is a small jump in $\Delta\nu$ as the N_{TB} phase is entered, in keeping with its first-order character. Within the N_{TB} phase the mean splitting increases slightly as the temperature is reduced. To show the correlation between the residual quadrupolar splitting and the diffusion anisotropy we plot one against the other in Figure 5 at the same temperatures. In the N phase there is a near linearity between $D_{||}/D_{\perp}$ and $\Delta\nu$; this is not quite so apparent in the N_{TB} phase largely because the quadrupolar splittings are distributed over a rather small range. In addition, the slopes of the plots in the two nematic phases are apparently different.

To take the relationship between these two properties further we recall that Chu and Moroi [25] have shown that the diffusion anisotropy for rod-like mesogens is related to the orientational order parameter, S , for the molecular long axis. Their starting point is for the individual diffusion coefficients, $D_{||}$ and D_{\perp} , which are written as

$$D_{//} = d(1 - S) + S\tilde{D}_{//} \quad (2)$$

and

$$D_{\perp} = d(1 - S) + S\tilde{D}_{\perp} \quad (3)$$

Here the tilde over \tilde{D} indicates that this diffusion tensor is for a perfectly ordered mesogenic cluster. The lower case d denotes the scalar component of the tensor \tilde{D} and is related to its trace, although this should be independent of the nematic orientational order. These equations satisfy two limiting states, first for the isotropic phase when S vanishes and secondly when S is unity. The ratio of the two equations gives the diffusion anisotropy as

$$D_{//}/D_{\perp} = \{(1 + 2\gamma) + 2(1 - \gamma)S\} / \{(1 + 2\gamma) - (1 - \gamma)S\}, \quad (4)$$

where γ is $\tilde{D}_{//}/\tilde{D}_{\perp}$ and for a rod-like molecule of length L and width w , this ratio is $\pi w/4L$.

However, by defining the anisotropy in the diffusion tensor as $(D_{//} - D_{\perp})/(D_{//} + 2D_{\perp})$ [26] then the anisotropy, R , is found to be linear in the order parameter, that is

$$R = \{(1 - \gamma)/(1 + 2\gamma)\}S. \quad (5)$$

To test Equation (5) requires knowledge of the orientational order parameter and the determination of this for an odd liquid crystal dimer, such as CB7CB-d₄, presents a challenge. Part of the challenge results from the flexibility of the heptane spacer linking the two cyanobiphenyl mesogenic groups. This can be overcome, in part, by setting the C-D axes in a rigid fragment of the molecule. Since the methylene fragment is attached to a cyanobiphenyl group this allows us to determine the order parameter for the para-axis of this mesogenic group, at least approximately [23]. Values determined for S in the nematic phase at the same temperatures as for the diffusion anisotropies have been used to produce the results shown in Figure 6 which clearly shows the linear dependence of R on S passing through the origin, as expected. From the slope of the straight line through the data for the nematic phase the optimum value of γ was found to be 0.129. The value for γ of 0.129 corresponds to a length-to-breadth ratio of about 6.1, we shall return to this shortly.

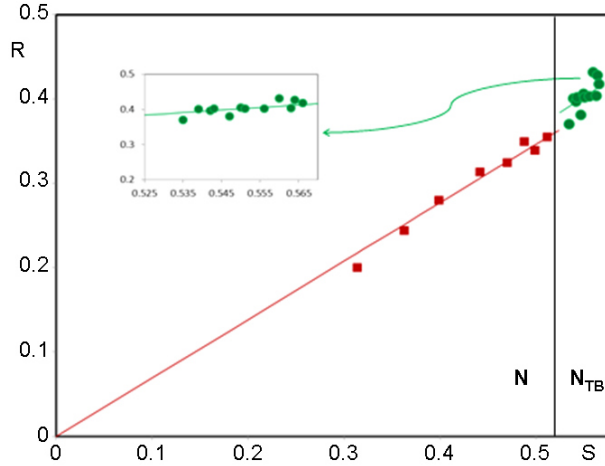


Figure 6. (colour online) The dependence of the diffusion anisotropy, R , on the orientational order parameter, S , for a mesogenic group of CB7CB in the nematic (■) and twist-bend nematic (●) phase determined at the same temperatures. The linear dependence, predicted by both the Chu-Moroi theory [25] and the Hess-Frenkel-Allen theory [26], in the nematic phase is shown as the red line. In addition the predictions of the extended versions of these theories in the twist-bend phase are also given as the green line.

At this stage we should note that the much later theory of Hess, Frenkel and Allen [26], based on an affine transformation, yields initially the diffusion tensor of perfectly aligned hard ellipsoids although the dependence on the orientational order was subsequently introduced through an ‘educated guess’. This gives the dependence of the anisotropy of the diffusion tensor on the order parameter as

$$R = \{(1 - Q^2)/(1 + 2Q^2)\}S, \quad (6)$$

where Q is the molecular anisotropy defined by L/w . Thus although the linear dependence of R on S is the same as that of Chu and Moroi [25] the relationship of the slope to the molecular anisotropy is quite different. From our experimental value of the slope the value of Q^2 is equal, necessarily, to 0.129 which gives L/w as about 2.8. This suggests a significant difference by a factor of 2.2 in the values predicted by the two theories. In principle these different values of L/w offers a way of seeing which of the two theories is the more reliable. The use of our experimental results to provide such a test is not straight forward however because the theories are for uniaxial molecules whereas the liquid crystal dimer CB7CB has molecules which are bent and flexible. To determine their shape and dimensions is clearly a challenging task but at this stage we have decided to adopt a simple approach. The CB7CB molecule is taken in its ground state with the spacer in its all-trans conformation and to allow for rotation about the spacer. This yields a shape resembling a cylinder with cones at either end; here molecular models suggest a total length of $\sim 28\text{\AA}$ and with the maximum cone width of $\sim 16\text{\AA}$ and the cylinder width of $\sim 3\text{\AA}$. These lead to a value for L/w of \sim

2.4 which is close to the value found from our experimental results analysed with the Hess-Frenkel-Allen theory and significantly smaller than that obtained with the Chu-Moroi theory. This conclusion is consistent with the results of molecular dynamics simulations studies of hard ellipsoids. [26]

We now seek to include the results for the twist-bend nematic phase to see if they are also consistent with the Chu-Moroi or the Hess-Frenkel-Allen theory expressed in Equations (5) and (6). However, the question is which orientational order parameter to use, that defined with respect to the director, nS , or that defined with respect to the helical axis, hS , to which it is tilted. It might seem natural to use hS since in our experiments the diffusion anisotropy is measured with respect to the helical axis, as is the order parameter. None the less since both theories are based on the use of the director frame it seems reasonable to start with the diffusion tensor expressed in this frame and to transform it into the helical frame. In the director frame the principal components of the uniaxial diffusion tensor are ${}^nD_{//}$, ${}^nD_{\perp}$ and ${}^nD_{\perp}$; the Euler angles needed to transform the director to the helical frame are φ , the azimuthal angle, obtained by rotating about the director axis and θ_0 , the polar angle, made by the director with respect to the helical axis. The angle θ_0 , which is a defining quantity of the N_{TB} , is also known as the conical or tilt angle [5]. In general the diffusion tensor in the helical frame contains five independent elements and the scalar component. This number is reduced to just one by averaging over the azimuthal angle φ which results from the diffusion of the molecules along the helical axis. As expected the diffusion tensor, ${}^h\mathbf{D}$, obtained by this diffusional averaging is uniaxial and the two components are

$${}^hD_{//} = d + ({}^nD_{//} - d)\mathcal{P}_2(\cos\theta_0) \quad (7)$$

and

$${}^hD_{\perp} = d + ({}^nD_{\perp} - d)\mathcal{P}_2(\cos\theta_0). \quad (8)$$

We progress from this by using Equations (2) and (3) relevant for the Chu-Moroi approach to replace the components in the director frame, ${}^nD_{//}$ and ${}^nD_{\perp}$. This gives

$${}^hD_{//} = d + (\tilde{D}_{//} - d){}^nSP_2(\cos\theta_0) \quad (9)$$

and

$${}^hD_{\perp} = d + (\tilde{D}_{\perp} - d){}^nSP_2(\cos\theta_0), \quad (10)$$

where the order parameter with respect to the director is denoted by nS . The product, ${}^nSP_2(\cos\theta_0)$, because of the uniaxiality in both frames is equivalent to the order parameter in the helical frame, hS . This leads to the following results for the diffusion coefficients in the twist-bend nematic phase

$${}^hD_{||} = d + (\tilde{D}_{||} - d) {}^hS \quad (11)$$

and

$${}^hD_{\perp} = d + (\tilde{D}_{\perp} - d) {}^hS, \quad (12)$$

as had been anticipated. The diffusion anisotropy, hR , is then given by

$${}^hR = \left\{ \frac{(1-\gamma)}{(1+2\gamma)} \right\} {}^hSP_2(\cos\theta_0) = \left\{ \frac{(1-\gamma)}{(1+2\gamma)} \right\} {}^hS \quad (13)$$

which is the analogue of the expression for nematics given in Equation (5). Since the order parameter hS in the twist-bend nematic phase is also available from 2H NMR experiments for CB7CB-d₄ [3] we are able to test the prediction in Equation (13). The dependence of the diffusion anisotropy on the order parameter in the N_{TB} phase is shown as the green circles in Figure 6. It is apparent that in this plot the points are confined to a relatively small area because the order parameter in the twist-bend nematic phase does not change significantly. [3] As a consequence the linearity of the data is not as impressive as in the N phase where both the diffusion anisotropy and the order parameter change significantly. However, the linearity of the results shown in the inset allows γ to be determined as 0.109 giving L/w as approximately 7.2 close to the value found in the nematic phase. It is likely that the increase in the molecular anisotropy could be a result of the narrow range of data but might be caused by the influence of the change in the phase structure. Again this intriguing possibility must await more precise measurements of the diffusion coefficients before it is possible to discuss the behaviour of the diffusion anisotropy with any certainty.

The similarity of the Chu-Moroi and Hess-Frenkel-Allen theories for the diffusion anisotropy of the nematic phase suggests that their predictions for the twist-bend nematic phase might also be comparable. To confirm this expectation we have derived R for the twist-bend nematic phase using the Hess-Frenkel-Allen theory. The starting point for deriving the diffusion anisotropy, hR , in the twist-bend nematic phase from the Hess-Frenkel-Allen theory [26] is Equations (7) and (8). These require the principal components of the diffusion tensor in the director frame together with its scalar component:

$${}^nD_{pa} = \alpha D_0 Q^{-2/3} \{ Q^2 - (2/3)(Q^2 - 1)(1 - {}^nS) \}, \quad (14)$$

$${}^nD_{pe} = \alpha D_0 Q^{-2/3} \{ 1 + (1/3)(Q^2 - 1)(1 - {}^nS) \}, \quad (15)$$

and

$$d = \alpha D_0 Q^{-2/3} (2 + Q^2). \quad (16)$$

The parameters α and D_0 do not appear in the anisotropy and so are not needed here but are defined in [26]. The anisotropy hR is found to be

$$\begin{aligned} {}^hR &= \{(1 - Q^2)/(1 + 2Q^2)\} {}^nSP_2(\cos\theta_0), \\ &= \{(1 - Q^2)/(1 + 2Q^2)\} {}^hS. \end{aligned} \quad (17)$$

The slope of the ${}^hR - {}^hS$ plot for the N_{TB} phase of 0.109 yields a value for L/w of about 3.0 which is close to that found from the results in the N phase of 2.8. The results and their analysis found for the N_{TB} phase match those for the N phase which to some extent is consistent with the results for other properties such as the orientational order. [27]

It is not always the case that the orientational order parameter is available for the nematic and twist-bend nematic phases. However, it may still be possible to determine the order parameter and the conical angle from the diffusion anisotropy with the aid of Equations (13) and (17). To use these results to determine nS and θ_0 from the temperature dependence of ${}^hD_{//}/{}^hD_{\perp}$ in the N_{TB} phase we need a function to describe their temperature dependence. It has been suggested in an earlier study of the order and conical angle of CB7CB [27] that Haller-like functions might be suitable and this proved to be the case. Thus the temperature dependence of the order parameter with respect to the director is written as

$${}^nS(T) = \{1 - y(T/T_{ref})\}^z, \quad (18)$$

where T_{ref} denotes T_{NI} in the nematic phase and T_{NtbN} in the twist-bend nematic phase. The analogous expression for the conical angle which only applies in the N_{TB} phase is

$$\theta_0(T) = \theta(0) \{1 - y_{\theta}(T/T_{NtbN})\}^{\beta}, \quad (19)$$

in each of these expressions there are, at most, three fitting parameters. Clearly to determine these requires a significant number of accurate data points which presents a formidable experimental challenge but one that should be accepted.

To characterise quantitatively the temperature dependence of translational diffusion coefficient in the different phases, we fit our data to the Arrhenius law

$$D(T) = D_0 \exp\{-E_0/RT\}. \quad (20)$$

A significant difference between the activation energies for the two diffusion coefficients in the nematic phase (see Table 1) is, as we have seen, partly attributed to the temperature variation of the orientational order parameter. The average activation energy in this phase, defined as

$$E_{A,av} = \frac{E_{A,\parallel} + 2E_{A,\perp}}{3}, \quad (21)$$

is not very different from that in the isotropic phase, in accord with analogous results obtained in nematic phases of calamitic mesogens; [28, 29] as found for CB7CB, for all of those cases the relation $E_{A,av} \approx E_{A,iso}$ holds as well as the inequalities $E_{A,\parallel} < E_{A,iso} < E_{A,\perp}$. In contrast, the activation energies increase significantly in the N_{TB} phase and most dramatically for diffusion along the symmetry axis or helix axis. This increase can be attributed to the effect of tilting the director

Table 1. The Arrhenius activation energies, E_A , for the diffusional processes in the I, N and N_{TB} phases of CB7CB.

Phase	$E_{A,\parallel}$ (kJ/mol)	$E_{A,\perp}$ (kJ/mol)
I	44.3	
N	33.8	50.1
N_{TB}	52.4	54.9

with respect to the helix axis which is parallel to the magnetic field; [17] this is similar to the behaviour found in chiral smectogens exhibiting the SmA-SmC* transition. [18] Assuming that the layer structure does not change abruptly between the two smectic phases, the difference in the activation energy was ascribed to the tilt of the director in the heliconical structure of the SmC* phase. [18]

The dependence of the translational diffusion coefficient in the twist-bend nematic phase on the diffusion time, Δ , has been investigated by performing experiments with diffusion times in the range from 800 ms to 160 ms at 94 °C. These gave single exponential decays and essentially the same values of the diffusion coefficients, namely $D_{\parallel} = 3.1 \times 10^{-11} \text{ m}^2/\text{s}$ and $D_{\perp} = 1.0 \times 10^{-11} \text{ m}^2/\text{s}$,

for diffusion along and normal to the magnetic field direction. The average molecular displacements along the gradient direction can be calculated from the relation

$$\langle r \rangle = \sqrt{2D\Delta}; \quad (22)$$

here $\langle r \rangle$ is the average displacement and D is the diffusion coefficient along the gradient direction. No boundary effect has been found, limiting the average domain dimension R_d by the conditions $R_d > 7\mu m$ or $R_d \ll 2\mu m$. [21] In other words, R_d is either larger than the largest displacement explored leaving, on average, molecules travelling in a single domain, or the molecules diffuse crossing a large number of small domains of different handedness

The dependence of the diffusion coefficient in the measurement directions has been carried out by measuring the diffusion along the X and Y directions of the laboratory frame. The diffusion coefficient determined for different directions and different diffusion times was consistent to within the experimental error. These results confirm that the diffusion tensor measured is uniaxial; the local biaxiality is averaged during the diffusion process. Analogous results have been obtained by measuring diffusion in the heliconical SmC* phase; also, in this case, the diffusion coefficient measured perpendicular to the helical pitch is independent of the direction of the measurement. [18]

An alternative view of the influence of the translational diffusion along the heliconical axis of the N_{TB} phase on the symmetry of the quadrupolar tensor is provided by the analysis given by Luz et al. [13] for the analogous problem in the N* phase. That is as the molecules diffuse along the helix axis they experience a rotation in the director orientation. According to this analysis the diffusion would average the biaxiality to zero in the N_{TB} phase if the inequality

$$D_{||} > \frac{p^2 \delta\Delta\nu}{2\pi^2} \quad (23)$$

is satisfied. Here p is the pitch of the heliconical helix, $\Delta\nu$ is the quadrupolar splitting and $\delta\Delta\nu$ is the biaxiality in the plane orthogonal to the helix axis. The biaxiality depends on the quadrupolar splitting along the helix axis, $\Delta\nu_{ZZ}$, and the conical angle θ_0 ; this is given approximately by

$$\delta\Delta\nu = \Delta\nu_{ZZ} \left[\frac{3 \sin^2 \theta_0}{2 - 3 \sin^2 \theta_0} \right], \quad (24)$$

where the two parameters Δv_{ZZ} and θ_0 are already known for the dimer CB7CB. [3,23] We have used the following values of the properties determined at approximately 30°C to estimate the RHS of Equation (24): $p = 8 \times 10^{-9} \text{m}$; $\Delta v_{ZZ} = 48 \times 10^3 \text{ s}^{-1}$ and $\theta_0 = 25^\circ$. The last two properties are used to estimate the biaxiality in the quadrupolar splitting as $17.6 \times 10^3 \text{ s}^{-1}$ this shows the RHS of the inequality to be $6 \times 10^{-15} \text{ m}^2 \text{ s}^{-1}$. This is much smaller than the diffusion coefficient which we have measured to be $3 \times 10^{-11} \text{ m}^2 \text{ s}^{-1}$ and this significant inequality demonstrates that the biaxiality in the quadrupolar splitting will be averaged to zero in the twist-bend nematic phase of CB7CB by the translational diffusion.

Another point to be discussed concerns the small change in the diffusion coefficients on passing from the nematic to the twist-bend nematic phase. The results reported here represent an essentially continuous behaviour in the molecular translational diffusion on crossing between the nematic

phases and also that the diffusion in the N_{TB} phase remains nematic-like, that is $\frac{D_{//}}{D_{\perp}} > 1$. However

this behaviour is in contrast to our results shown in Appendix 1 which clearly demonstrate that the macroscopic rotational viscosity, related to the field-induced director dynamics, does become much larger on passing from the N to the N_{TB} phase. This behaviour does, however, agree with the angular dependent ^2H NMR measurements made by Hoffmann et al. [11] for the nonyl homologue, CB9CB, where the rotational viscosity increases in the N_{TB} phase with respect to the nematic phase. Assuming that the higher macroscopic viscosity in the N_{TB} phase with respect to the nematic phase corresponds to slow molecular translational diffusion, Hoffmann et al. [11] discuss their experimental results on the assumption that the molecular displacement is too slow to produce any averaging of the biaxiality in the residual quadrupolar splitting tensor. Based on the uniaxiality of the N_{TB} phase it is then argued that the phase deviates from the structure proposed for it by Dozov. [5]

As we have seen our results for the translational diffusion coefficient of the lower homologue CB7CB, actually contradict this result; the diffusion coefficient does not change abruptly from the nematic to the N_{TB} phase, as we report in Figure 3, remaining fast enough to average the biaxiality of the residual quadrupolar splitting to zero. Of course, this result does not prove the presence of a heliconical structure in the phase but rather confutes the hypothesis of slow translational diffusion in the N_{TB} phase, in particular compared with that in the higher nematic phase. In other words although the twist-bend nematic phase is locally biaxial the residual quadrupolar tensor is found to be uniaxial in the ^2H NMR experiment because of the rapid diffusion along the helix axis. This does not, of course, show that the N_{TB} does not have a heliconical structure but, in the spirit of Ockham,

it does show that until further evidence is obtained there is no need to reject the proposed heliconical structure of the twist-bend nematic phase.

Other evidence in support of the view that the macroscopic viscosity can differ from the microscopic one in liquid crystals, comes from the smectic A phases of the cyanobiphenyls. Even though the smectic A phase, in contrast to the nematic phase, does not reorient in a relatively high magnetic field, [30], still a rather continuous behaviour of the diffusional process is found, on moving from the nematic to the smectic A phase, as shown by experiments [30, 31] as well as computer simulations. [32] In this sense, the N_{TB} nematic phase is similar to the SmA phase, indeed recently an analogy has been proposed between the two phases. [33, 34]

5. Conclusions

The translational diffusion coefficients have been measured in the isotropic, nematic and twist-bend nematic phases of the odd liquid crystal dimer CB7CB. Our results show an essentially continuous diffusional behaviour between the two nematic phases, both phases showed uniaxial diffusion tensors, the diffusion anisotropy remains greater than unity and increases as the temperature decreases also in the N_{TB} phase. However, at the N to N_{TB} phase transition a small but significant increase of $D_{//}$ is observed. We tentatively interpret this increase as the result of an increase of the orientational order with respect to the magnetic field in the presence of a relatively small conical angle [35,27].

Of particular interest is the observation that the translational diffusion along the heliconical axis remains quite fast. Indeed it is sufficiently fast to average the residual quadrupolar splitting to yield a uniaxial quadrupolar tensor in the twist-bend nematic phase as observed experimentally for this intrinsically biaxial phase.

The variation of the diffusion coefficient anisotropy is found to be correlated with the residual quadrupolar splitting in both N and N_{TB} phases. In addition, the associated variation with the orientational order of a mesogenic arm of the dimer is found to be in good accord with the predictions of both the Chu-Moroi [25] and Hess-Frenkel-Allen [26] theory of monomers for the nematic phase but the weaker variation in the twist-bend nematic phase makes it more difficult to test their extended theories here. Comparison of the molecular anisotropy extracted from the diffusion coefficient anisotropy for the N phase with an estimate of that for CB7CB suggests that the Hess-Frenkel-Allen theory is more reliable than the Chu-Moroi theory.

Concerning the supramolecular heliconical structure of the N_{TB} phase, indirect evidence of its formation may be inferred from the increase in the activation energy for the diffusion process on

moving from the N to the N_{TB} nematic phase, as reported in Table 1. This increase can be associated with the director tilt with the consequent twisting of the director analogous to what happens at the transition to the SmC^* phase formed by chiral mesogens. Indeed it should be possible to determine the heliconical angle and orientational order parameter from precise measurements of the diffusion tensor by applying the theoretical models developed here. This possibility will be the aim of further investigations also in other systems exhibiting the N_{TB} phase.

Appendix 1. Symmetry of the residual quadrupolar splitting tensor and dynamics of the field-induced director/helix axis alignment for N and N_{TB} phases of CB7CB-d₄

The symmetry of the residual quadrupolar splitting tensor was determined by placing the sample of CB7CB-d₄ in a controlled porous glass, CPG 3000B.[3] This allowed the director in the N phase and the helix axis in the N_{TB} phase to be randomly distributed by surface forces with respect to the 7.05 T magnetic field of the NMR spectrometer. The resultant spectral powder patterns measured revealed that in both the nematic phase and the twist-bend nematic phase the quadrupolar tensors are uniaxial with respect to the director and the helix axis, respectively. [3] In addition to these experiments we also studied a monodomain sample of CB7CB-d₄ in the N and N_{TB} phases; here we take the opportunity to report such results for the first time. In these experiments the short NMR tube is horizontal but the director in the N phase and the helix axis in the N_{TB} phase are aligned parallel to the magnetic field which is vertical. [23] Rotation of the NMR tube about its horizontal axis by 90° will rotate the director/helix axis so that it is orthogonal to the magnetic field; however, the positive anisotropic magnetic susceptibility means that these two axes will tend to be aligned parallel to the magnetic field. In fact in the N_{TB} phase it is also required that the conical angle is less than the magic angle 54.74°. Following the sample rotation the NMR spectra can be measured in a continuous time-resolved NMR experiment.[36]

The measurement of the ²H NMR spectra of CB7CB-d₄ was made in a Varian Infinity Plus 300 spectrometer using a quadrupolar echo sequence (²H Larmor frequency 46 MHz). The 90° pulse was of 5μs duration and the spectra were acquired using a spectral width of 150 kHz saved in a 4K memory file.

In the nematic phase at 109 °C the spectrum is found to remain unchanged as we can see from the stack plot shown in Figure A1. The reason this occurs is that following the mechanical rotation of the sample which takes about 12 s the director is rapidly realigned by the magnetic field parallel to it which occurs during the first experiment. Clearly after the initial spectrum, subsequent acquisition of spectra also contains just a single doublet with the same splitting because the director orientation parallel to the field cannot change.

The situation for the twist-bend nematic phase at 90°C is clearly quite different as is apparent from the stack plot of spectra shown in Figure A2; the first few of these are shown more

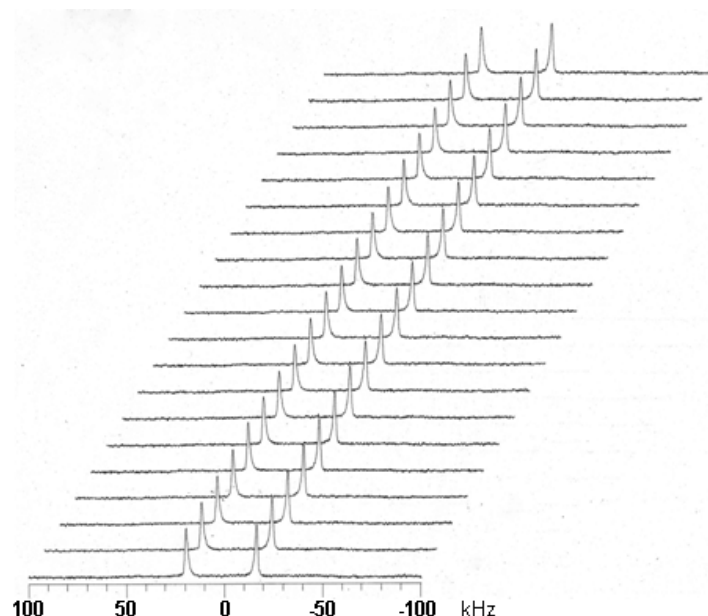


Figure A1. The time dependence of the ^2H NMR spectrum of CB7CB- d_4 in its nematic phase measured following the rotation of the sample by 90° at 109°C . The spectra were obtained using 160 transients with 40ms delay between transients. The time between successive spectra which contain single quadrupolar doublets was 12s. During this first period the director is aligned parallel to the magnetic field of 7.05T.

clearly in Figure A3. The first spectrum is seen to contain four quadrupolar doublets. The larger two of these result when the helix axis is parallel to the magnetic field. They were obtained simply by keeping the helix axis parallel to the field and there are two quadrupolar splittings because of the chirality of the twist-bend nematic phase. [3] The two smaller quadrupolar splittings having the sharper spectral lines appear after the sample had been rotated by 90° leaving the helix axis perpendicular to the magnetic field. The ratio of the quadrupolar splittings when the helix axis is parallel and perpendicular to the magnetic field is related to the symmetry of the residual quadrupolar splitting and hence the phase. [37] If this is uniaxial then the ratio of the quadrupolar splittings should be 2:1. From the initial spectrum shown in Figure A2 and enlarged in Figure A3 the prochiral splittings give the following ratios of 1.99:1 and 2.00:1 for the larger and the smaller residual quadrupolar splittings, respectively. This reveals, to within experimental error, the uniaxiality of the quadrupolar tensor

The spectra also contain information about the field-induced alignment process; [36] thus it is apparent from the spectral intensity between the two perpendicular lines that some of the helix axis is starting to be aligned by the magnetic torque at angles less than 90° . The significant width of these peaks shows that the helix axis is widely distributed as it rotates towards being parallel to the magnetic field. This alignment process continues as is apparent from the increase in the quadrupolar splitting between the broad peaks which now exceeds that between the sharp perpendicular peaks.

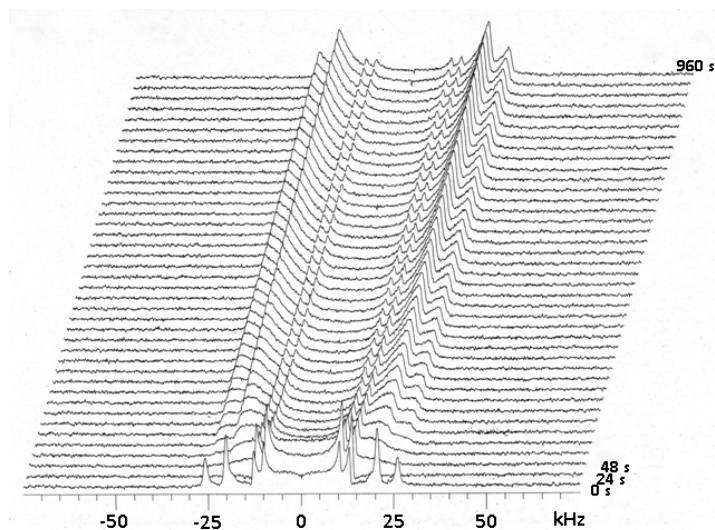


Figure A2. The time-dependence of the ^2H NMR spectrum measured for CB7CB- d_4 in its twist-bend nematic phase at 90°C . The strength of the aligning magnetic field is again 7.05 T and the initial spectrum was obtained by rotating the sample by 90° half way through the acquisition of the spectrum. The spectra were obtained using 256 transients with 80ms delay between transients. The two larger splittings result from the helix axis parallel to the magnetic field and the second two come from the magnetic field being essentially perpendicular to the helix axis. The time between recording two adjacent spectra is 24 s.

In the last spectrum shown in Figure A3 after 288s the inner perpendicular peaks are weak in intensity while that of the outer lines has grown significantly and the magnitudes of the two splittings indicate that the helix axis has been realigned parallel to the magnetic field. The fact that the peaks grow during the alignment process is interesting for it shows that the helix axis is not realigned as a monodomain. This is reminiscent of the alignment process for the director of a nematic with a positive anisotropic susceptibility when the aligning field is initially perpendicular to it. [36] The alignment progresses in the N_{TB} for some considerable time as is apparent from the stack plot shown in Figure A2.

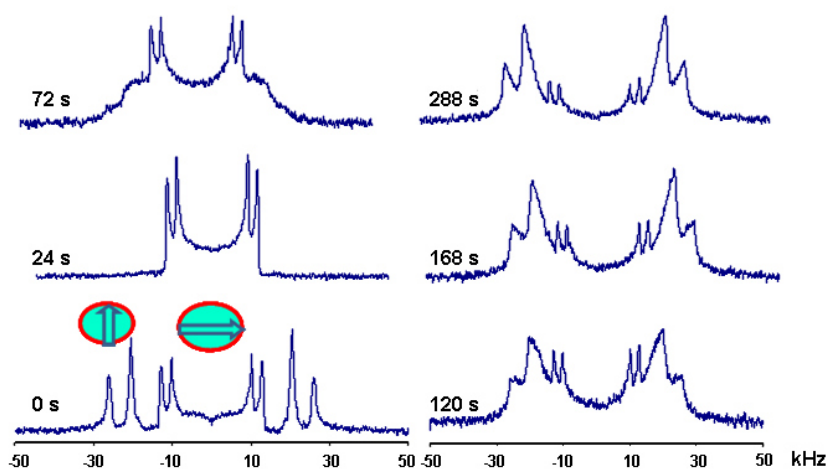


Figure A3. (colour online) A selection of the ^2H NMR spectra taken from the stack plot shown in Figure A2. This shows in more detail the time variation of the spectra as the helix axis is rotated from perpendicular to parallel to the magnetic field.

As might be expected the field-induced alignment of the helix axis in the twist-bend nematic phase of CB7CB-d₄ at lower temperatures is even slower. This can be seen from the stack plot, given in Figure A4, for the dimer in the N_{TB} phase at 80°C just 10°C than that shown in Figure A2. As for the results obtained at the higher temperature it is also possible to determine the symmetry of the residual quadrupolar tensor. The ratios of the prochiral, parallel and perpendicular residual quadrupolar splittings extracted from the initial spectra shown in Figures A4 and A5 are 1.98:1 and 2.00:1. Again, to within experimental error, these are equal to 2:1 thus showing that the magnetic tensors for twist-bend nematic phases are uniaxial in keeping with other measurements [3, 11]

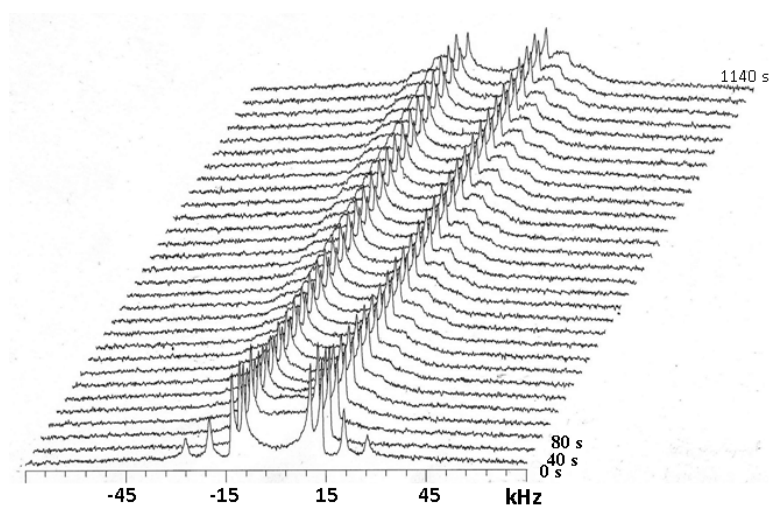


Figure A4. The stack plot for CB7CB-d₄ in its twist-bend nematic phase at 80°C; here the time between spectra is 40s. The spectra were obtained using 400 transients with 80ms delay between transients. It is clear that at this slightly lower temperature the rate of change in the spectra and hence the helix axis distribution is significantly reduced. However we note that the two quadrupolar doublets associated with the helix axis perpendicular to the magnetic field remain in place although there is a slight variation in their intensity.

Whereas the uniaxiality of the phase is unchanged at the lower temperature it is clear from the stack plot in Figure A4 that the dynamics of the field-induced rotation of the helix axis has slowed considerably. Indeed even at the end of the stack after the sample rotation the lines associated with the helix axis perpendicular to the magnetic field remain sharp. In marked contrast the four peaks associated with the helix axis parallel to the magnetic field are extremely broad. This again demonstrates that the helix axis is not aligned as a monodomain. [36] Indeed this is apparent from the variation in the spectral intensities and not simply from the location of the peaks.

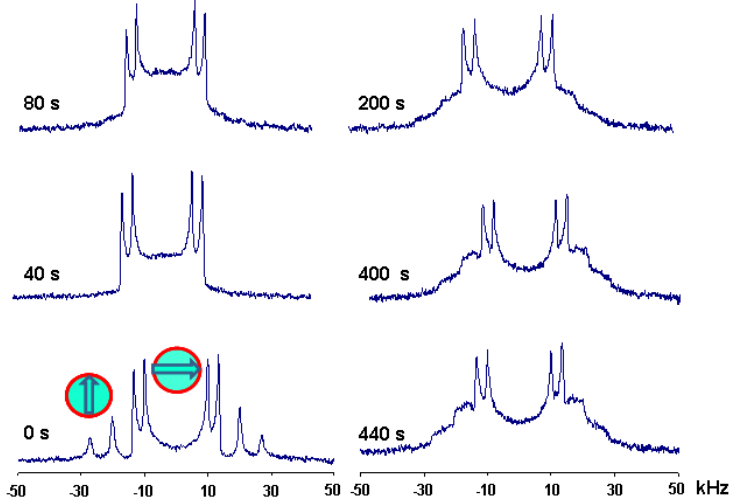


Figure A5. (colour online) A selection of spectra showing, in more detail, the time dependence of the ^2H NMR spectra of CB7CB- d_4 in the N_{TB} phase at 80°C . It is especially noticeable that although the perpendicular peaks remain sharp those associated with the helix axis parallel to the magnetic field are broad. This demonstrates the breadth of the helix axis distribution generated by the field-induced alignment of the director from perpendicular to parallel alignment.

It is difficult to make a quantitative comparison with how the field-induced helix dynamics change with temperature and indeed with other dynamic processes. However, we might start by first estimating the time taken for the spectra to adopt the same form at different temperatures. For example, at 90°C where the rotation is relatively fast we see that in Figure A3 after 72 s we find that the spectrum with sharp perpendicular and broad parallel peaks matches that at 80°C in Figure A5 after 440 s although it also resembles that at 400 s. Armed with the first two times, τ , we wish to estimate the activation energy to compare with those obtained from the temperature dependence of the diffusion coefficients. To do this we assume an exponential process

$$\tau = A \exp(-\Delta'/RT), \quad (\text{A1})$$

and solve the simultaneous equations for τ_1 and τ_2 at T_1 and T_2 , respectively. In this way we estimate that the activation energy, Δ' , is approximately 190 kJ/mol. This is about three times the value for the diffusion coefficients also in the twist-bend nematic phase. This difference is consistent with the fact that one involves director rotation whereas the other involves molecular translation.

Appendix 2. Proton Spectra and Diffusion Decays from ^1H NMR Diffusometry Experiments

Figure A6, shows a single-pulse proton NMR spectrum acquired in the nematic phase ($T=110\text{ }^\circ\text{C}$) and the first-row spectrum of the PFG STE-ME of two experiments performed in the nematic phase ($T=110\text{ }^\circ\text{C}$) and twist-bend nematic phase ($T=98\text{ }^\circ\text{C}$). The single pulse (90° pulse) spectrum was acquired with a single scan and a receiver gain set to 4. The PFG STE-ME experiments, to measure diffusion along the Z direction, were carried out by acquiring 24 scans with a receiver gain of 480 for each of the 32 gradient steps, with a repetition time between scans of 4 s (T_1 was estimated to be about 1 s).

As shown in the figure the proton spectrum is dominated by dipolar couplings, in particular from the aromatic moieties, forming doublets with splittings of 8-10 kHz.

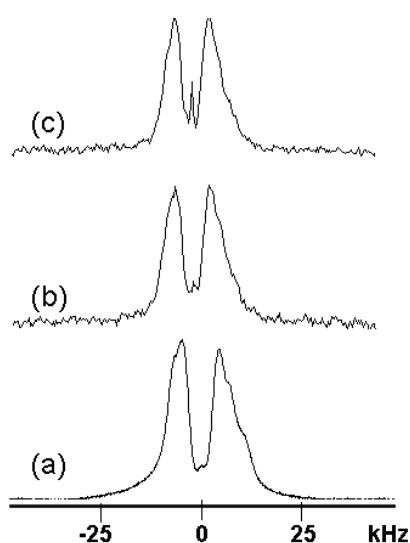


Figure A6. Examples of proton NMR spectra acquired in the nematic and twist-bend nematic phase of the CB7CB sample. (a) single pulse spectrum ($T=103\text{ }^\circ\text{C}$), (b) first row of the PFG STE-ME performed along the Z direction in the nematic phase at $T=110\text{ }^\circ\text{C}$, (c) first row of the PFG STE-ME performed along the Z direction in the twist bend nematic phase at $T=98\text{ }^\circ\text{C}$. Further experimental details are discussed in the text.

As can be seen in Figure A6, despite signal loss with respect to the single pulse acquisition, the spectra of the PFG STE-ME show the same features and quite a good signal-to-noise ratio also for a limited number of scans and consequently a relatively short time for the experiment (about 40 min).

In Figure A7 we show the signal decays as a function of the strength of the field-gradient for the two experiments performed in the nematic and twist-bend nematic phase. As is clear the quality of the data allowed the determination of the translational diffusion coefficient along the gradient direction with an experimental error between 4 and 2% evaluated as the standard deviation coming from three repetitions of the experiment.

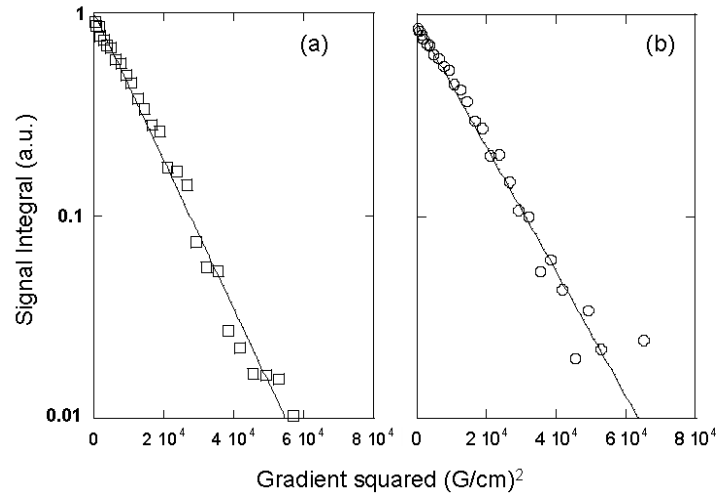


Figure A7. The linearised Stejskal-Tanner plot of the echo signal versus the squared gradient strength, measured along the Z direction in (a) the nematic phase at $T=110$ °C and (b) the twist-bend nematic phase at $T=98$ °C.

References

- [1] Šepel M, Lesac A, Baumeister U, Diele S, Nguyen HL, Bruce BW. Intercalated liquid-crystalline phases formed by symmetric dimers with an α,ω -diiminoalkylene spacer. *J Mat Chem*. 2007; 17: 1154-1165.
- [2] Panov VP, Nagaraj M, Panarin YuP, Kohlmeier A, Tamba MG, Lewis RA, Mehl GH, *Phys Rev Lett*. 2010; 105:167801.I
- [3] Cestari M, Diez-Berart S, Dunmur DA, et al. Phase behavior and properties of the liquid-crystal dimer 1'', 7''-bis(4-cyanobiphenyl-4'-yl) heptane,: A twist-bend nematic liquid crystal. *Phys. Rev. E*. 2011;84:031704.
- [4] Meyer RB. Structural problems in liquid crystal physics, Les Houches Summer School in Theoretical Physics. 1973 *Molecular Fluids*, eds. Balian R, Weil G., Gordon and Breach, New York 1976, 273-373.
- [5] Dozov I., On the spontaneous symmetry breaking in the mesophases of achiral banana-shaped molecule, *Europhys. Lett.* 2001; 56,247-253.
- [6] Chen D, Porada JH, Hooper JB, Klitnick A, Shen Y, Tuchband MR, Bedrov D, Walba DM, Glaser MA, MacLennan JE, Clark NA, Chiral heliconical ground state of nano scale pitch in a nematic liquid crystal of achiral molecular dimers, *Proc. Natl. Acad. Sci.*, 2013; 110: 15931-15936.
- [7] Greco C, Luckhurst GR, Ferrarini A, Enantiotropic discrimination and director organization of the twist-bend nematic phase, *Phys Chem Chem Phys*. 2013; 15: 14961.
- [8] Gorecka E, Salamonczyk M, Zep A, Poheca D, Welch C, Ahmed Z, Mehl G, Do the short helices exist in the nematic TB phase?, *Liquid Crystals*, 2015; 42: 1-7.
- [9] Vanakaras AG, Photinos DJ A molecular Theory of the Nematic-Nematic Phase Transitions in Mesogenic Dimers. *Soft Matter*, 2016;12:2208-2220.
- [10] Mandle RJ et al. Apolar Bimesogens and the Incidence of the Twist-Bend Nematic Phase. *Chem. Eur. J*. 2015;21:8158-8167.
- [11] A. Hoffmann, A.G. Vanakaras, A. Kohlmeier, G.H. Mehl, D.J. Photinos, On the structure of the Nx phase of symmetric dimers: inferences from NMR, *Soft Matter*, 2015; 11: 850-855
- [12] Chidichimo G, Yaniv Z, Vaz NAP, Doane JW, Biaxial ordering, self-diffusion, and helix-distortion effects on 2H NMR spectral patterns from cholesteric liquid crystals. *Phys Rev. A* 1982; 25:1077-1083.
- [13] Luz Z, Poupko R, Samulski ET, Deuterium NMR and molecular ordering in the cholesteryl alkanoate mesophases, *J Chem Phys*; 1981, 74,: 5825-5837.
- [14] Henderson PA, Imrie CT, Methylene-linked liquid crystal dimers and the twist-bend nematic phase. *Liq. Cryst.* 2011;38:1407-1414.
- [15] Krüger CJ, Diffusion in thermotropic liquid crystals. *Phys Rep*. 1982; 82: 229-269.
- [16] Dvinskikh SV, Furó I, Nuclear magnetic resonance studies of translational diffusion in thermotropic liquid crystals, *Russ. Chem. Rev.*, 2006, 75 497-506.
- [17] Cifelli M, Domenici V, Dvinskikh SV, Glogarova M, Veracini CA, Translational self-diffusion in the synclitic to anticlinic phases of a ferroelectric liquid crystal, *Soft Matter*. 2010; 6: 5999-6003.
- [18] Cifelli M, Domenici V, Dvinskikh SV, Veracini CA, Zimmermann H. Translational self-diffusion in the smectic phases of ferroelectric liquid crystals: an overview. *Phase Transitions*. 2012; 85: 861-871.
- [19] Dvinskikh SV, Furó I. Anisotropic self-diffusion in nematic, smectic-A, and reentrant nematic phases. *Phys Rev E*. 2012; 86: 031704.
- [20] Cifelli M, Domenici V, Kharkov BB, Dvinskikh SD. *Mol. Cryst. Liq. Cryst.*, 614; 2015: 30–38.
- [21] W.S: Price, Pulsed-Field Gradient Nuclear Magnetic Resonance as a Tool for Studying Translational Diffusion: Part 1. Basic Theory, *Concepts Magn. Reson.*, 1997; 9;299-336.
- [22] van Vaals JJ, Bergman AH, Optimization of eddy current compensation, *J. Magn. Reson*. 1990; 90: 52-70 .
- [23] Beguin L, Emsley JW, Lelli M, Lesage A, Luckhurst GR, Timimi BA, Zimmermann H. The chirality of a twist-bend nematic phase identified by NMR spectroscopy. *J Phys Chem B*. 2012;116:7940-7951.
- [24] Emsley JW, Lelli M, Lesage A, Luckhurst GR. A comparison of the conformational distributions of the achiral symmetric liquid crystal dimer CB7CB in the achiral nematic and chiral twist-bend nematic phases. *J Phys Chem B*. 2013;117:6547-6557.
- [25] Chu KS, Moroi DS. Self-diffusion in nematic liquid crystals. *J. Phys Colloq*. 1975; 33: C1-99-101.
- [26] Hess S, Frenkel D, Allen MP, On the anisotropy of the diffusion tensor in nematic liquid crystals: test of a modified affine transformation model via molecular dynamics. *Mol. Phys*. 1991, 74: 765-774.
- [27] Jokisaari JP, Luckhurst GR, Timimi BA., Zhu J., Zimmermann H., Twist-bend nematic phase of the liquid crystal dimer CB7CB. Orientational order and conical angle determined by ^{129}Xe and ^2H NMR spectroscopy *Liq Cryst*, 2015; 42: 708-721.
- [28] Dvinskikh SV, Furó I, Anisotropic self-diffusion in the nematic phase of a thermotropic liquid crystal by ^1H -spin-echo nuclear magnetic resonance. *J. Phys. Chem.*, 2001, 115(4): 1946-1950 .
- [29] Dvinskikh SV, Furó I, Zimmermann H, Maliniak A, Anisotropic self-diffusion in thermotropic liquid crystals studied by ^1H and ^2H pulse-field-gradient spin-echo NMR. *Phys. Rev. E*, 2002, 65: 061701.
- [30] Cifelli M, McDonald PJ, Veracini CA, Translational self diffusion in 4-n-octyloxy-4'-cyanobiphenyl (8OCB) exploited with a static field gradient H-1 NMR diffusometry approach. *Phys Chem Chem Phys*. 2004; 6: 4701-4706.

-
- [31] Dvinskikh SV, Furó I., Sandstrom D, Maliniak A, Zimmermann H, Deuterium stimulated-echo-type PGSE NMR experiments for measuring diffusion: Application to a liquid crystal. *J. Magn. Reson.* 2001; 153: 83-91.
- [32] Prampolini G, De Gaetani L., Computational study through atomistic potentials of a partial bilayer liquid crystal: structure and dynamics. *Soft Matter.* 2009; 5: 3517–3526.
- [33] Meyer C, Dozov I, Analogy between the twist-bend nematic and the smectic A phase and the coarse-grained description of the macroscopic N_{TB} properties. *Soft Matter.* 2016; 10: 574-580.
- [34] Imrie CT, Luckhurst GR, Liquid Crystal Dimers and Oligomers, *Handbook of Liquid Crystals, 2nd Ed. Volume 7*, Ed. J.W. Goodby, P.J. Collings, T. Kato, C. Tschierske, H.F. Gleeson, P. Raynes 2014, Chapter 5 Page 169, Wiley-VCH Verlag GmbH & Co. KGaA
- [35] Meyer C, Luckhurst GR, Dozov I, The temperature dependence of the heliconical tilt angle in the twist-bend nematic phase of the odd dimer CB7CB. *J Mater Chem C*, 2015, 3, 318-328.
- [36] Sugimura A, Luckhurst GR, Deuterium NMR investigations of field-induced alignment of nematic liquid crystals. *Prog NMR Spect.* 2016; 94-95: 37-74.
- [37] Luckhurst GR, Biaxial nematic liquid crystals: Fact or fiction? *Thin Solid Films*, 2001; 393: 40-52.